

# Nanoindentation

2025 Characterization of Materials Summer School  
4<sup>th</sup> September 2025, EPFL

**Sándor Lipcsei**, PhD student

*Laboratory of Mechanical Metallurgy (LMM), EPFL*

# Why?

- Swiss army knife of nanomechanics, most widely used method (> 20000 publications);
- High significance in market and industrial development (DIN EN ISO 14577 standard since 2002);
- High-throughput method, experimentally simple, financially forgiving;
- It was developed in Switzerland by J. Pethica and W.C. Oliver in 1982 at Brown – Boveri (now ABB);

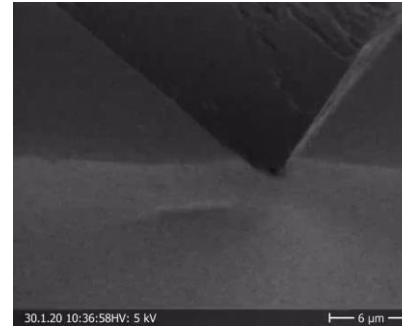
# How?



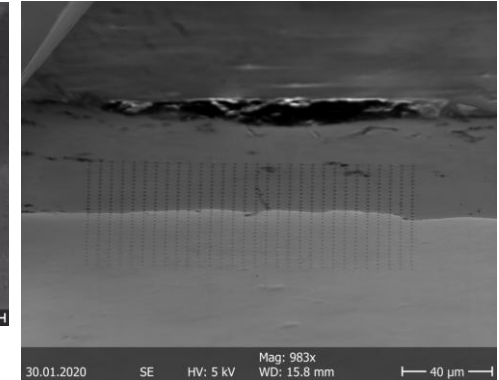
HYSITRON



Micro Materials  
Excellence in Nanomechanics



<https://alemnis.com/test-methods/mapping/>



## MICROHARDNESS TESTS WITH PENETRATION DEPTHS LESS THAN ION IMPLANTED LAYER THICKNESS

J. B. Pethica

Brown Boveri Research Center, 5405 Baden, Switzerland

### ABSTRACT

A special microhardness tester capable of making indentations as little as a few tens of nanometres deep is described. Ion implanted layer hardness may thus be directly measured. The depth of penetration is continuously monitored and, knowing the indenter shape, hardness (mean contact pressure) values may be calculated at all stages of an indentation. The results show that hardness is generally higher for smaller deformed volumes; surface preparation conditions are important. Nitrogen ion implantation of a number of mechanically polished stainless steels has been found to have a small or insignificant effect on the hardness. Cemented tungsten carbide showed a reduction of hardness in the first few hundred nm of surface.

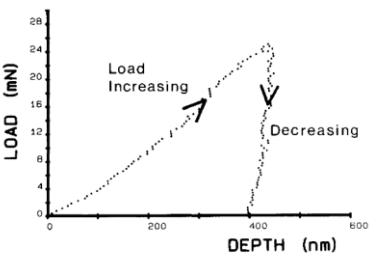
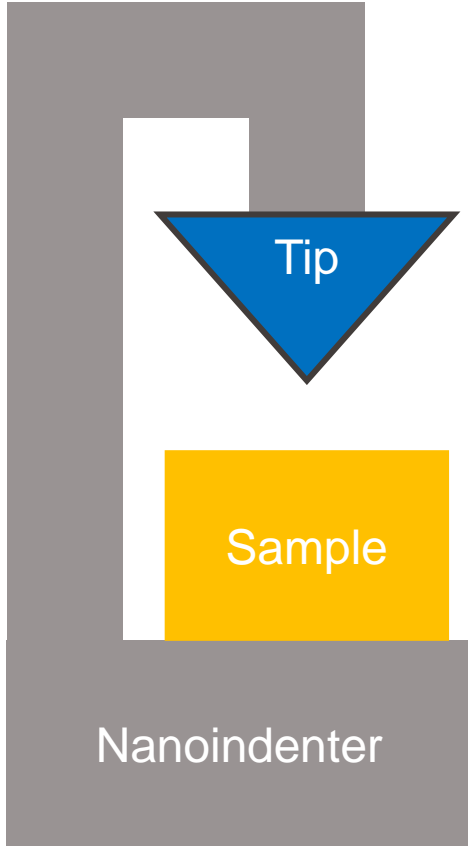
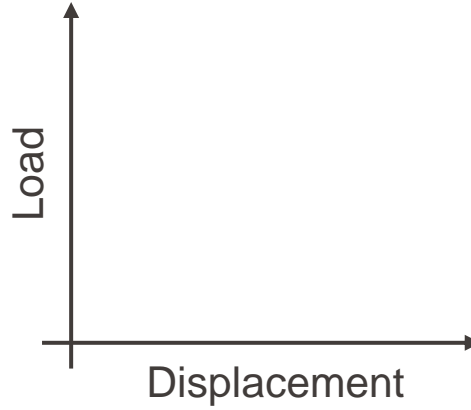


Fig. 2. Typical variation of indentation depth with load.

# Why?



# How?



# What?

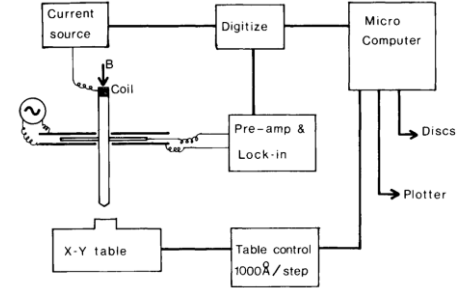
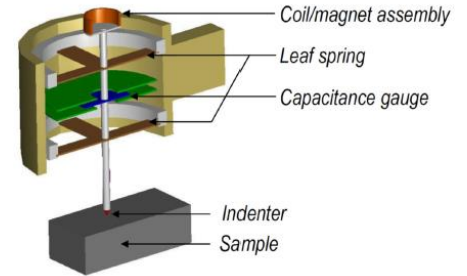


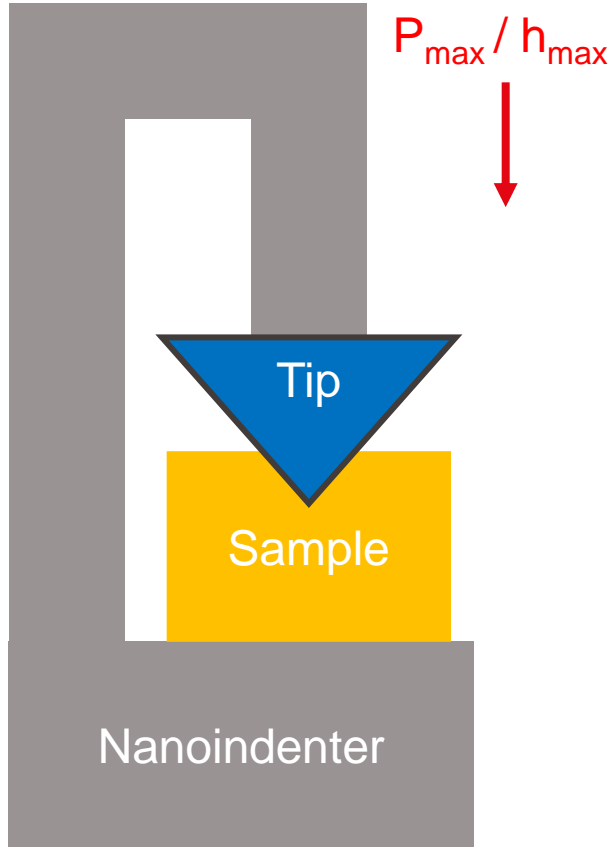
Fig. 1. Apparatus Schematic.

*J. B. Pethica (1982)*

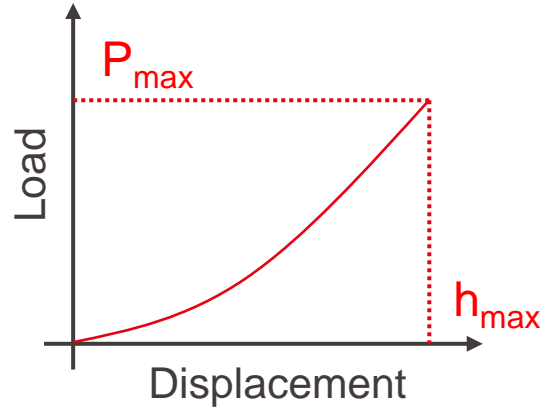


*KLA iMicro (based on the original design)*

# Why?



# How?



# What?

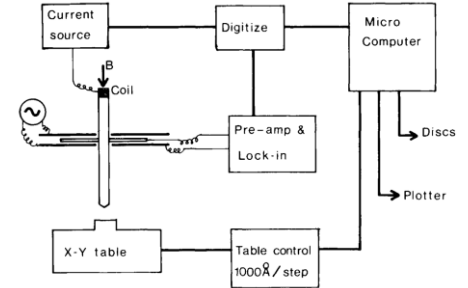
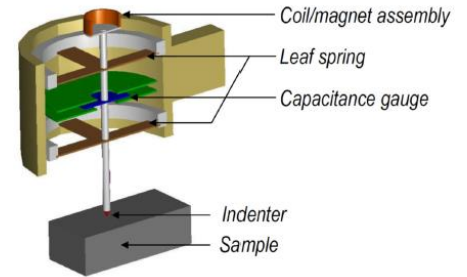


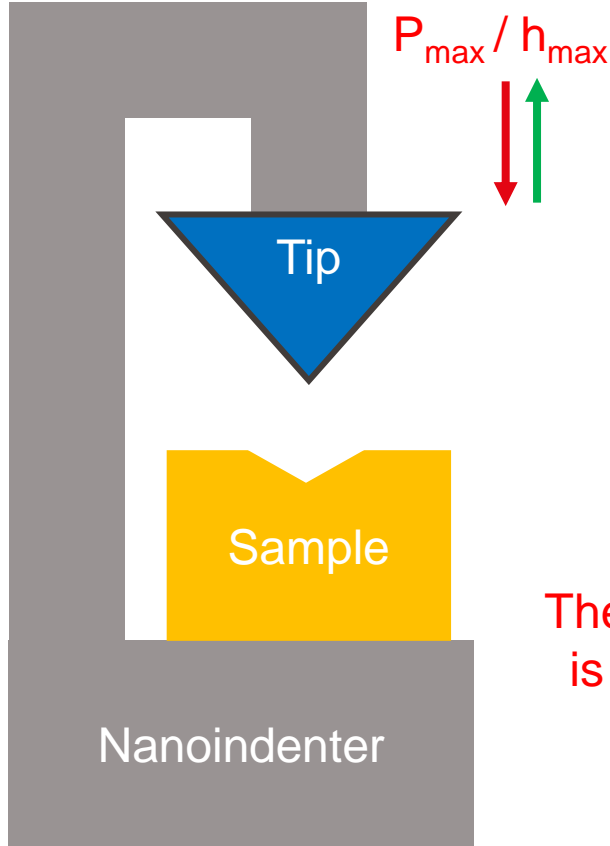
Fig. 1. Apparatus Schematic.

*J. B. Pethica (1982)*

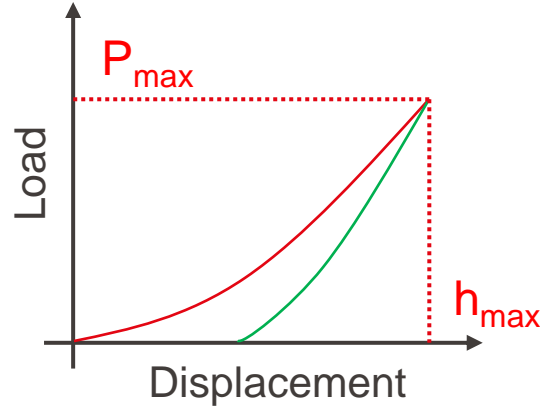


*KLA iMicro (based on the original design)*

# Why?



# How?



The experimental procedure is simple, the stress field / evaluation is complex!

# What?

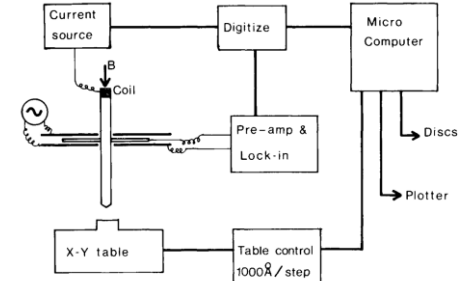
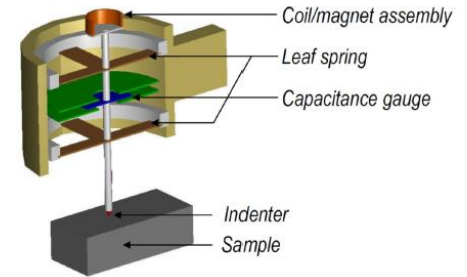


Fig. 1. Apparatus Schematic.

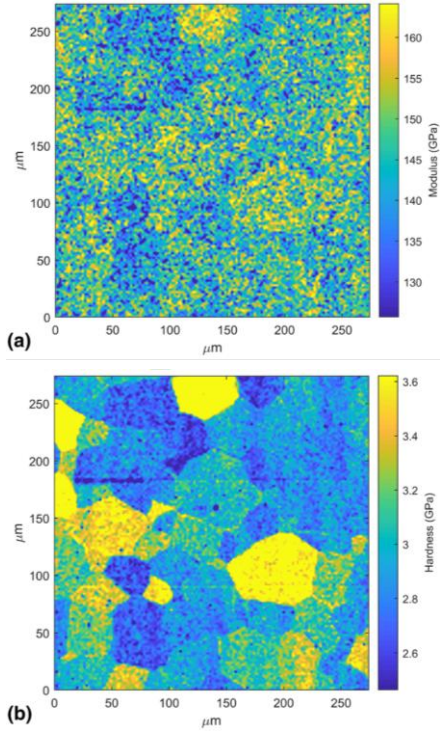
*J. B. Pethica (1982)*



*KLA iMicro (based on the original design)*

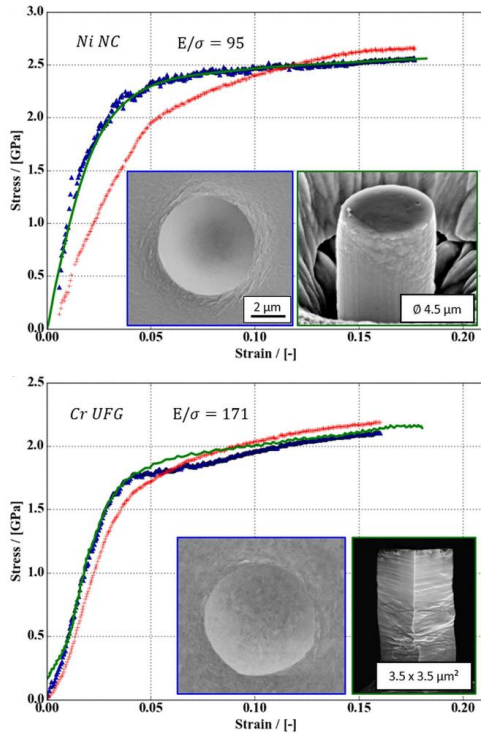
# Why?

## Hardness, Modulus



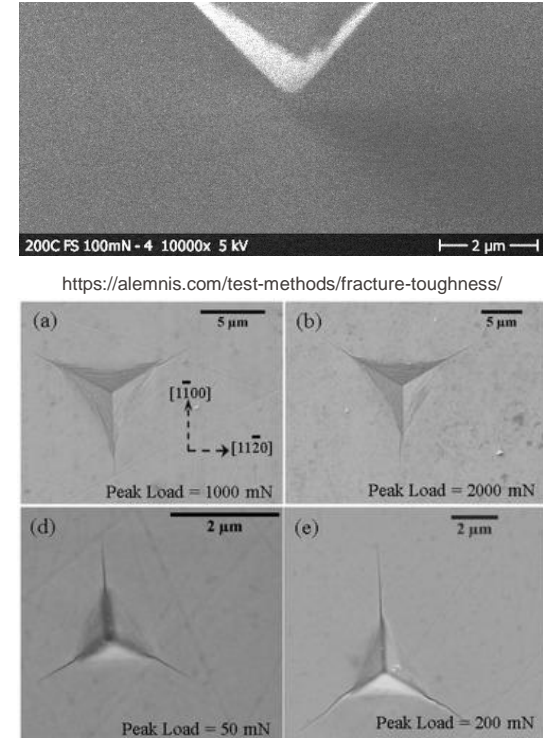
# How?

## Stress-strain curves



# What?

## Fracture toughness



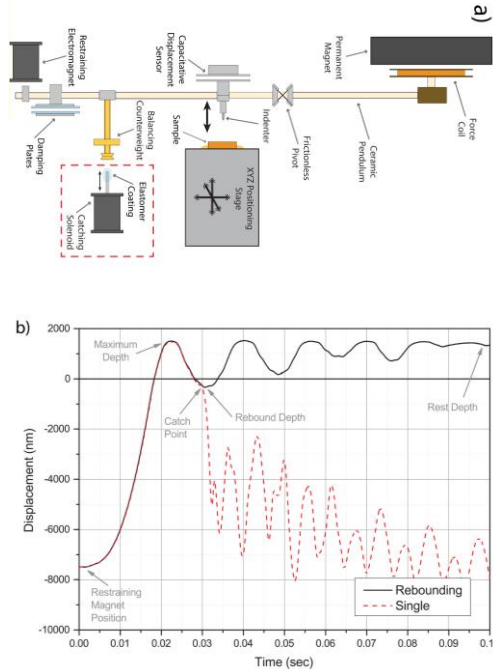
Magazzeni, Christopher M., et al. "Nanoindentation in multi-modal map combinations: a correlative approach to local mechanical property assessment." *Journal of Materials Research* 36.11 (2021): 2235-2250.

Leitner, A., V. Maier-Kiener, and D. Kiener. "Essential refinements of spherical nanoindentation protocols for the reliable determination of mechanical flow curves." *Materials & Design* 146 (2018): 69-80.

Datye, Amit, Udo D. Schwarz, and Hua-Tay Lin. "Fracture toughness evaluation and plastic behavior law of a single crystal silicon carbide by nanoindentation." *Ceramics* 1.1 (2018): 198-210.

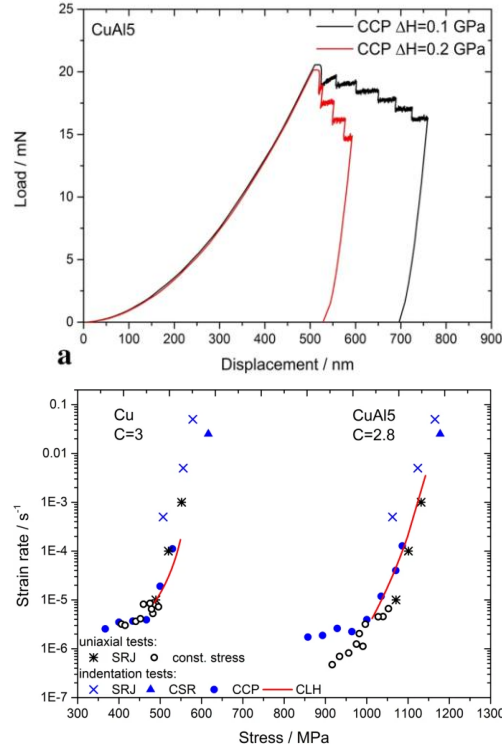
# Why?

## Impact testing



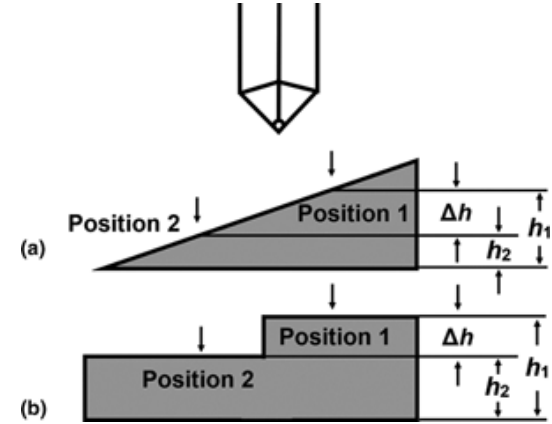
# How?

## Creep properties



# What?

## Coefficient of thermal expansion

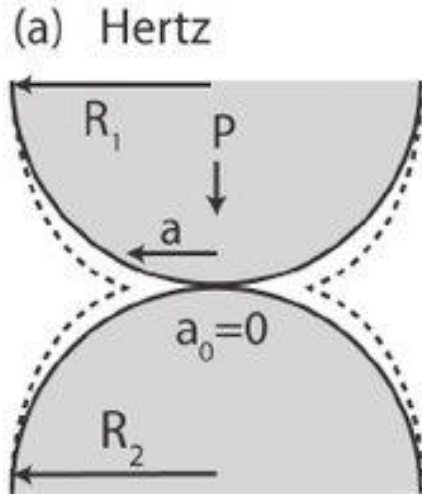


Samples	Linear CTEs ( $\times 10^{-6} \text{ } ^\circ\text{C}^{-1}$ )
Al (56.0 $\mu\text{m}$ ) this work	22.9 $\pm$ 5.3
Al (15 $\mu\text{m}$ ) [29]	24.6
Bulk Al [30]	24.0
Ti (90.3 $\mu\text{m}$ ) this work	11.6 $\pm$ 1.5
Ti (3.2 $\mu\text{m}$ ) [29]	8.79 (transverse direction), 9.16 (rolling direction)
Bulk Ti [31]	9.5

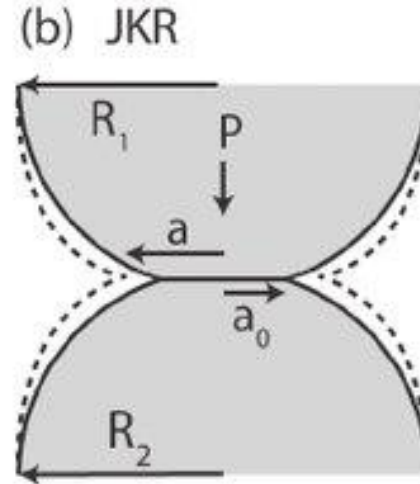
Wheeler, Jeffrey M., J. Dean, and T. W. Clyne. "Nano-indentation for high strain rate testing: The influence of rebound impacts." *Extreme Mechanics Letters* 26 (2019): 35-39.

Minnert, Christian, and Karsten Durst. "Nanoindentation creep testing: Advantages and limitations of the constant contact pressure method." *Journal of Materials Research* 37.2 (2022): 567-579.

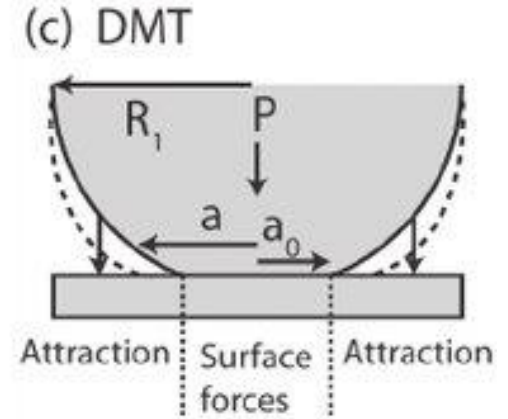
Qin, Yuanbin, et al. "Simple nanoindentation-based method for determining linear thermal expansion coefficients of micro-scale materials." *Journal of Materials Research* 35.23-24 (2020): 3202-3209.



- Elastic contact



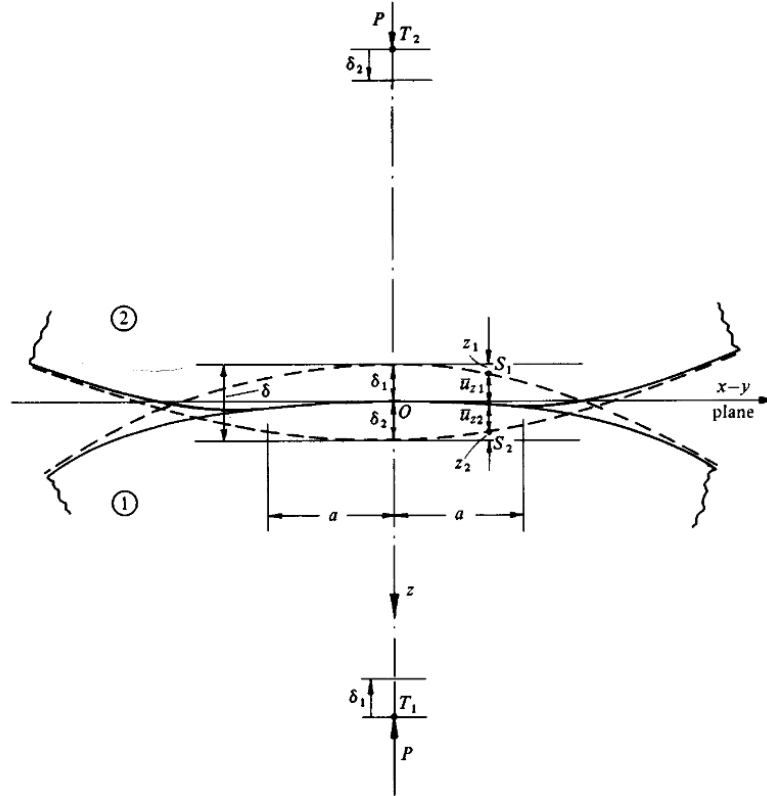
- Elastic contact  
- Adhesion



- Elastic contact  
- Adhesion  
- Van der Waals forces

None of these theories considers  
plasticity or time-dependent behaviour!

Fig. 4.2.



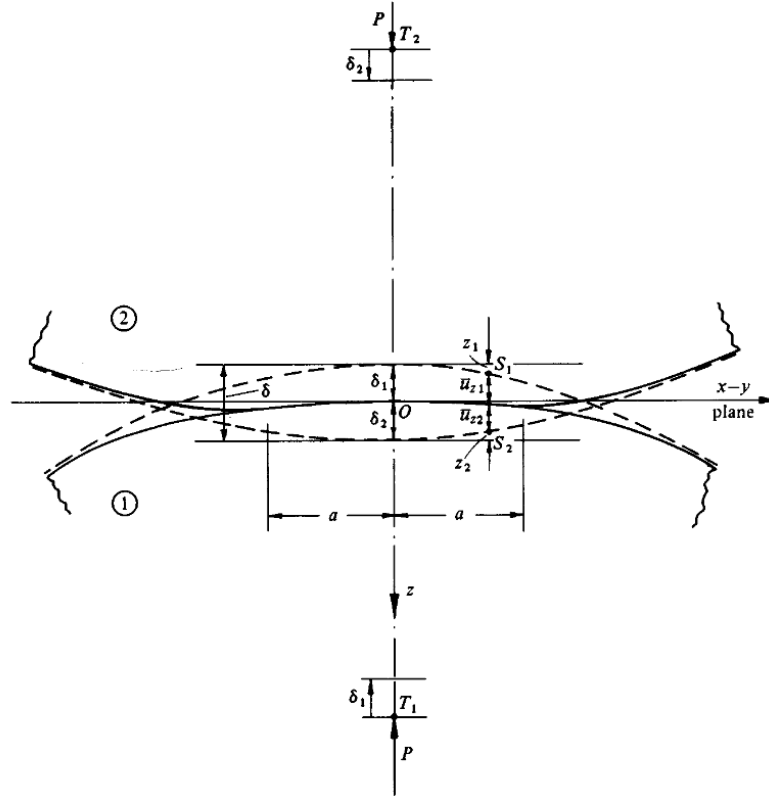
## Hertzian contact

### Assumptions:

- Material is isotropic and homogeneous;
- Deformation is linear – elastic;
- Each solid is infinitely large with respect to the deformed volume (they are considered elastic half-spaces);
- Surfaces are continuous and non-conforming;
- The contact is frictionless;

Most of the assumptions are not true generally speaking... so why should we study this problem? **It is a good starting point.**

Fig. 4.2.



Johnson, Kenneth Langstreth. *Contact mechanics*. Cambridge university press, 1987.

## Hertzian contact

By studying the local elastic displacements,  $\bar{u}_{z1}$  and  $\bar{u}_{z2}$  Hertz derived the expression for the approach of two distant points, i.e. the **total displacement** in the solids as

$$\delta_1 + \delta_2 = h = \left( \frac{9 F^2}{16 E_r^2 R^*} \right)^{\frac{1}{3}}$$

and the **radius of contact area**

$$a_c^2 = hR^*$$

where  $E_r$  is the **reduced modulus** and  $R^*$  is the **relative curvature** defined as

$$\frac{1}{E_r} = \left( \frac{(1 - \nu_1^2)}{E_1} + \frac{(1 - \nu_2^2)}{E_2} \right)$$

$$\frac{1}{R^*} = \frac{1}{R_1} + \frac{1}{R_2}$$

In the special case of a **sphere – plane contact**, i.e.  $R_2 = \infty$ :

$$F = \frac{4}{3} R E_r h^{\frac{3}{2}}$$

and since  $R \gg h_c$

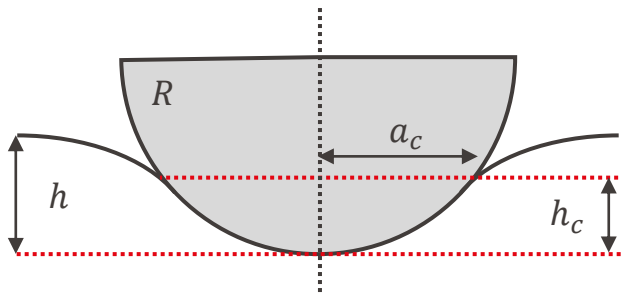
$$a_c^2 = 2Rh_c - h_c^2 \approx 2Rh_c$$

but also

$$a_c^2 = hR$$

meaning that

$$h_c = \frac{h}{2} = \frac{h_e}{2}$$



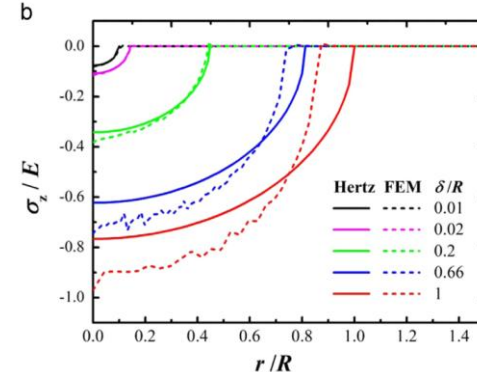
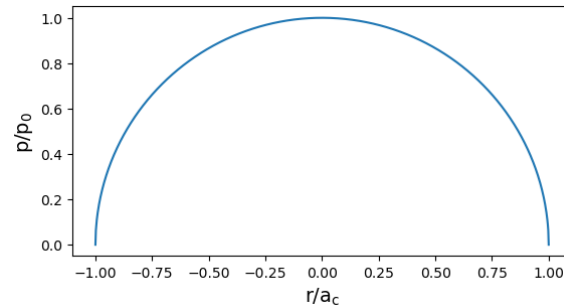
## Hertzian contact

Hertz also derived the maximum pressure as a function of the total load, resulting in

$$p_0 = \frac{3P}{2\pi a_c^2} = \frac{3}{2} p_{avg.}$$

which allows us to visualize the pressure – distribution proposed by Hertz:

$$p = p_0 \sqrt{1 - (r/a_c)^2}$$



Wu, Chen-En, Keng-Hui Lin, and Jia-Yang Juang. "Hertzian load–displacement relation holds for spherical indentation on soft elastic solids undergoing large deformations." *Tribology International* 97 (2016): 71-76.

## Sneddon (1965)

Unified the elastic theories and introduced the analysis of elastic – plastic materials, but only for **axially symmetric indenters**, namely defining

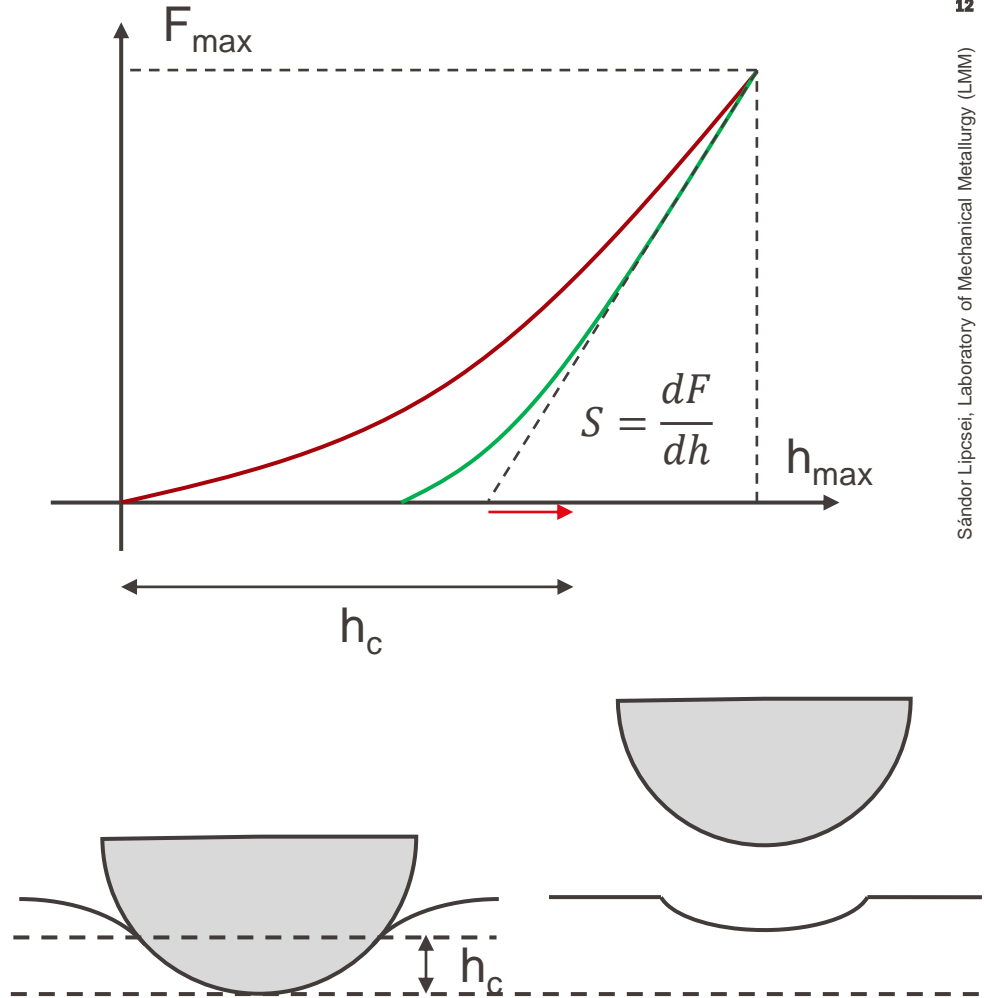
$$F = \varepsilon h^m$$

for the loading and unloading segment, where:

- $m = 1.0$ ,  $\varepsilon = 1$  for a flat punch;
- $m = 1.5$ ,  $\varepsilon = 0.75$  for a sphere;
- $m = 1.5$ ,  $\varepsilon = 0.75$  for a paraboloid;
- $m = 2.0$ ,  $\varepsilon = 0.72$  for a cone;

Sneddon also assumed that the recovery during unloading is completely elastic and therefore

$$h_c = h_{max} - \varepsilon F_{max} \frac{1}{S} \Big|_{F_{max}}$$



## Sneddon (1965)

Unified the elastic theories and introduced the analysis of elastic – plastic materials, but only for **axially symmetric indenters**, namely defining

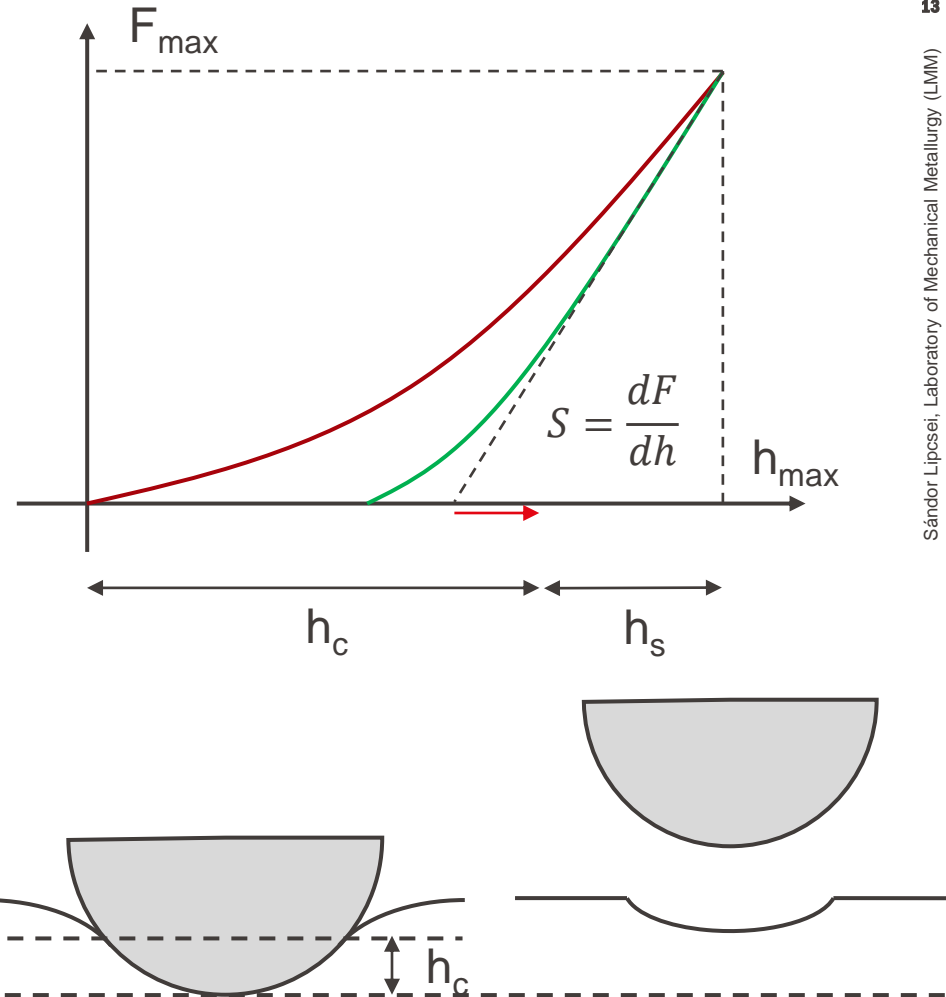
$$F = \varepsilon h^m$$

for the loading and unloading segment, where:

- $m = 1.0$ ,  $\varepsilon = 1$  for a flat punch;
- $m = 1.5$ ,  $\varepsilon = 0.75$  for a sphere;
- $m = 1.5$ ,  $\varepsilon = 0.75$  for a paraboloid;
- $m = 2.0$ ,  $\varepsilon = 0.72$  for a cone;

Sneddon also assumed that the recovery during unloading is completely elastic and therefore

$$h_c = h_{max} - \varepsilon F_{max} \frac{1}{S} \Big|_{F_{max}}$$



## Sneddon (1965)

Unified the elastic theories and introduced the analysis of elastic – plastic materials, but only for **axially symmetric indenters**, namely defining

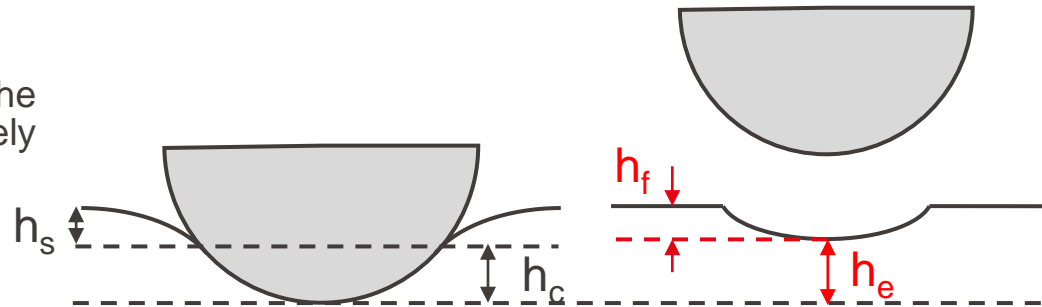
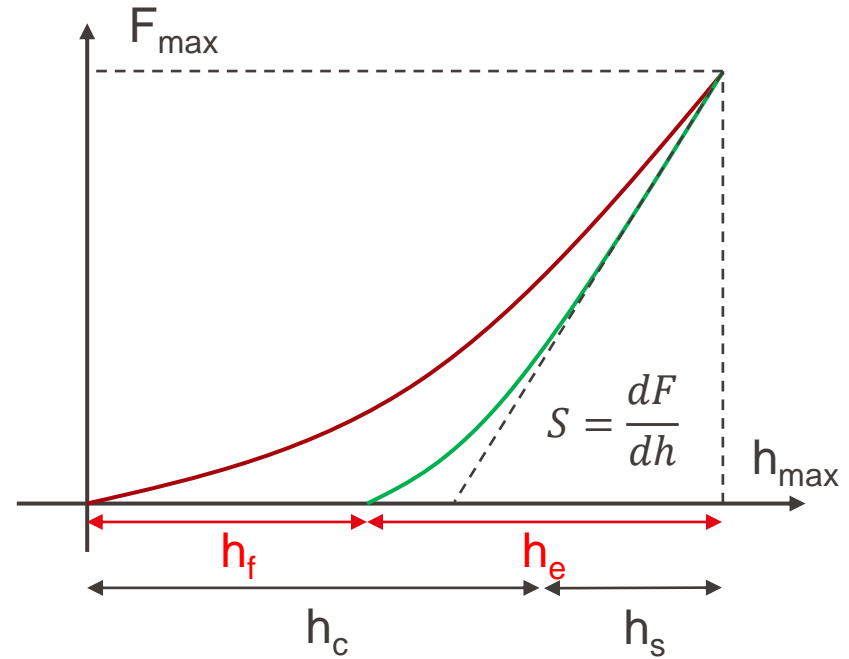
$$F = \varepsilon h^m$$

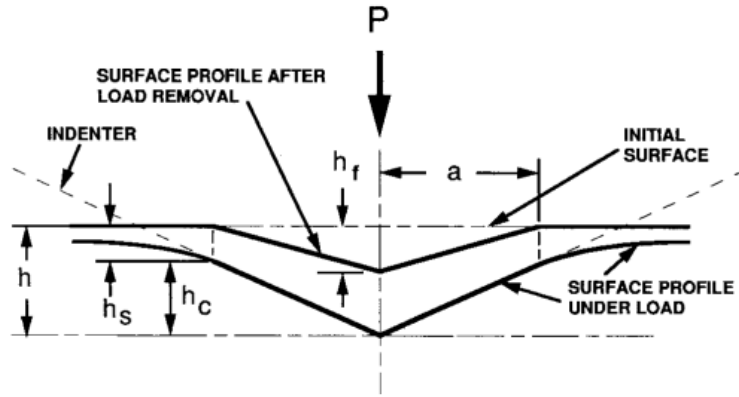
for the loading and unloading segment, where:

- $m = 1.0$ ,  $\varepsilon = 1$  for a flat punch;
- $m = 1.5$ ,  $\varepsilon = 0.75$  for a sphere;
- $m = 1.5$ ,  $\varepsilon = 0.75$  for a paraboloid;
- $m = 2.0$ ,  $\varepsilon = 0.72$  for a cone;

Sneddon also assumed that the recovery during unloading is completely elastic and therefore

$$h_c = h_{max} - \varepsilon F_{max} \frac{1}{S} \Big|_{F_{max}}$$





W.C. Oliver & G.M. Pharr (1992)

Unified theory for all elastic – plastic materials and for non axially symmetric indenters too:

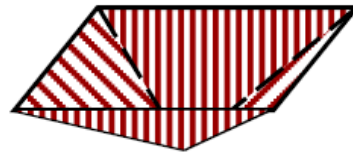
$$E_r = \frac{1}{\beta} \frac{\sqrt{\pi}}{2} \frac{S}{\sqrt{A_c}}$$

where  $\beta$  is a geometric correction for the corners of the indenters (Berkovich -  $\beta \approx 1.034$ ). Hardness was defined as

$$H = \frac{F_{max}}{A_c} \neq H_V = \frac{F}{A_d}$$



Projected area  
( $A_p$ )



Developed  
area ( $A_d$ )

# Know your setup...

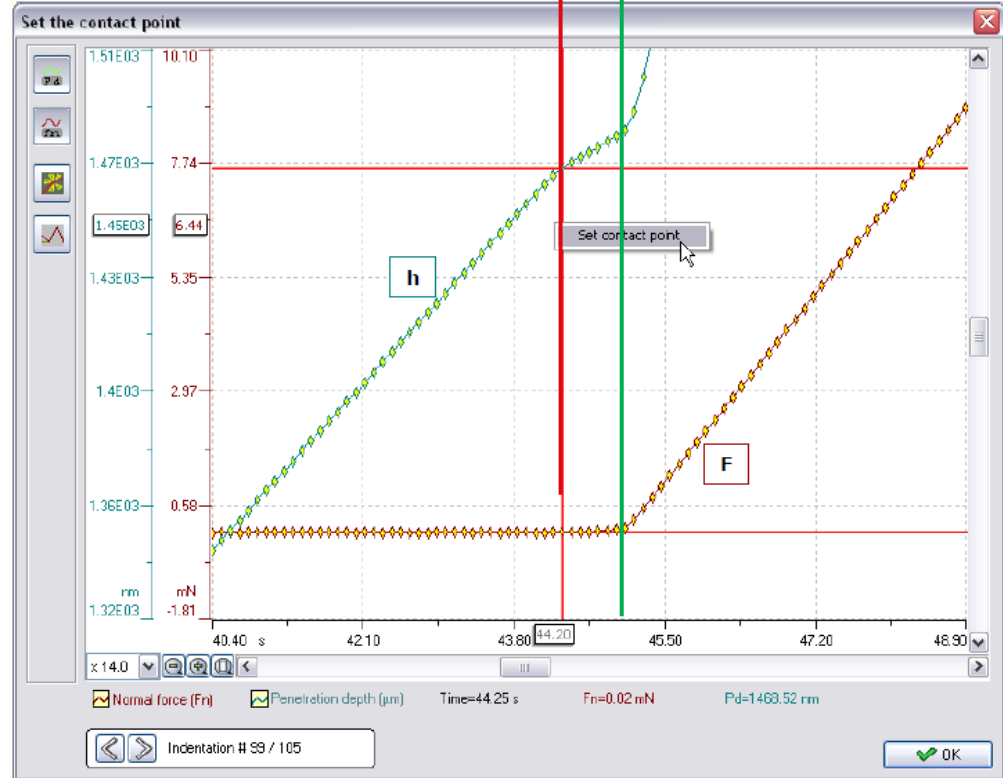
## Contact point detection

Automated algorithms can help to process the data, but the contact point detection is still challenging.

The reason for this is the same as for humans: there is no proper definition of the contact point.

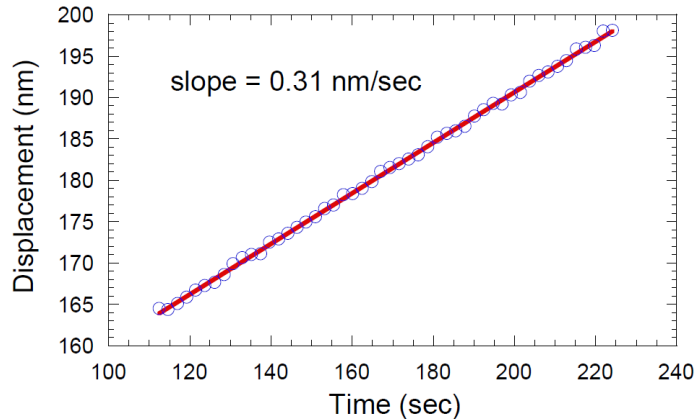
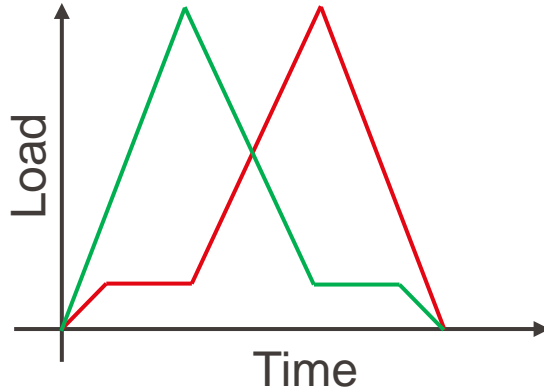
Methods:

- Normal method (stiffness criterion)
- First contact
- Effective zero - point



# Know your setup...

## Thermal drift & Mechanical vibrations



Thermal drift is usually measured when the tip is already (or still) in contact with the sample at a low load, in order to exclude any creep.

$$\Delta L = L_0 \alpha \Delta T$$

where  $\Delta L$  is the change in length,  $L_0$  is the initial length,  $\alpha$  is the coefficient of linear thermal expansion and  $\Delta T$  is the temperature difference.

### Example:

Frame length:  $L_0 = 300 \text{ mm}$

Aluminium:  $\alpha = 24 \cdot 10^{-6} / ^\circ\text{C}$

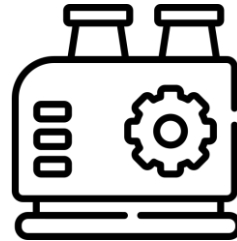
Variation of temperature:  $0.05^\circ\text{C} / \text{min}$

Variation of length: **346.5 nm / min**

# Know your setup...

## Thermal drift & Mechanical vibrations

Sources of mechanical vibrations:



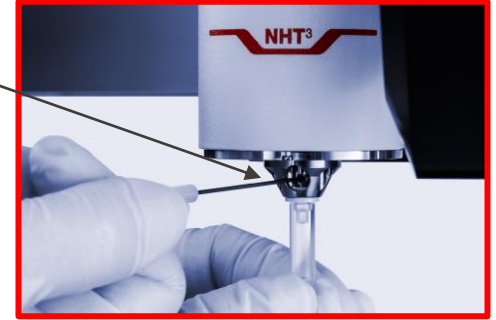
# Know your setup...

## Thermal drift & Mechanical vibrations

To minimize both: **Shielding & Dampening**

- Isolating your setup from the environment helps a lot (**enclosure**);
- **Top-referencing** is very useful too: instead of a frame size of 300 mm, one can reduce it to 5 or 10 mm;
- **Vibration-dampening tables** are essential against high-frequency vibrations;

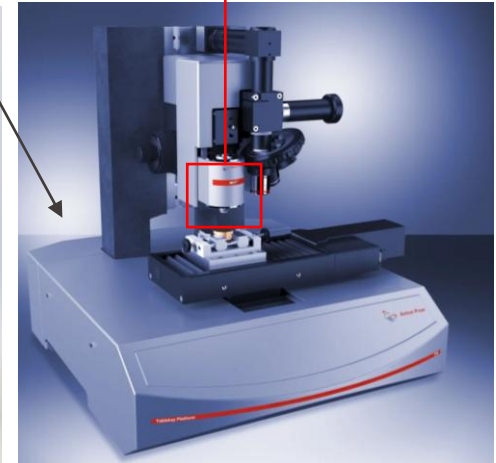
Reference ring  
(Top referencing)



Vibration-dampening base



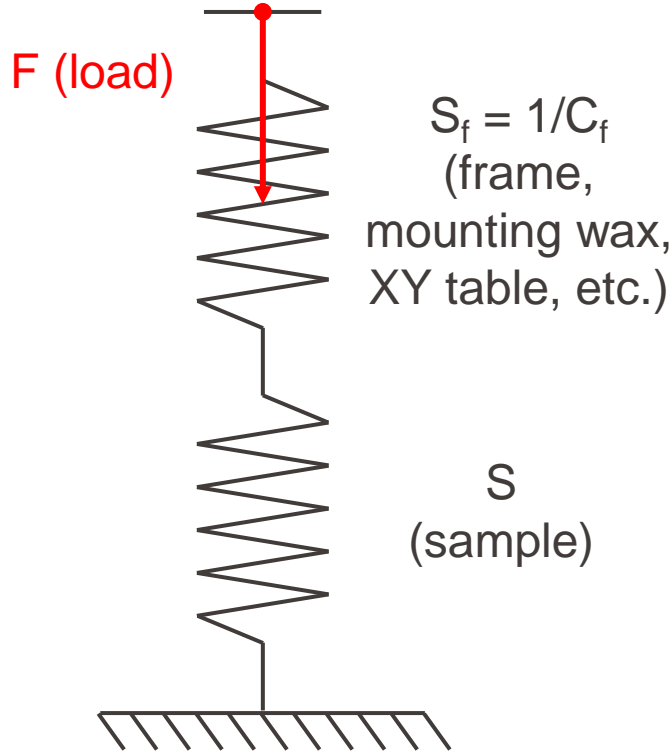
Bruker Hysitron TI 990



Anton Paar NHT<sup>2</sup> / NHT<sup>3</sup>

# Know your setup...

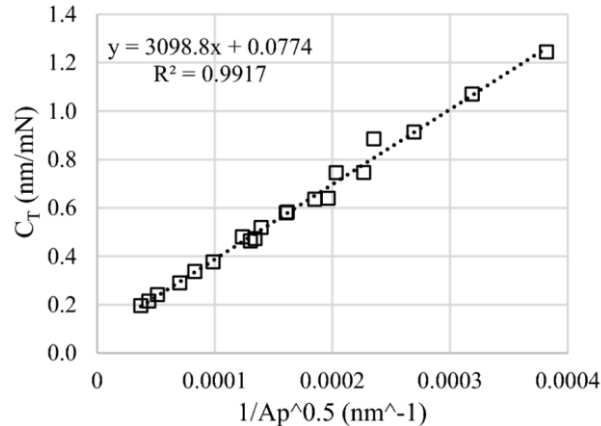
## Frame compliance



The total compliance is the sum of the frame and the sample compliance

$$C_t = C_s + C_f = \frac{\sqrt{\pi}}{2\beta} \frac{1}{E_r \sqrt{A_c}} + C_f$$

meaning that by **having a calibrated tip** one can also calibrate the frame compliance by **fitting a linear on  $C_t$  vs.  $1/\sqrt{A_c}$** .



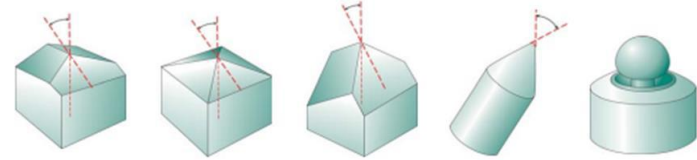
Chicot, Didier, et al. "Self-calibration in compliance and indenter tip defect for instrumented indentation." *Journal of Materials Research* 37.17 (2022): 2775-2792.

# Know your tip...

## Tip geometry

- Berkovich, cube-corner and conical tips are ideal for hard and stiff materials;
- Cube-corner being the sharpest is the best for fracture toughness measurements;
- Vickers is not ideal, because it's almost impossible to machine a four – sided pyramid with a sharp apex;

Indenting Tips Summary



	Berkovich	Vickers	Cube-Corner	Cone (angle $\psi$ )	Sphere (radius R)
<b>Features</b>					
Shape	3-sided pyramid	4-sided pyramid	3-sided pyramid w/ perpendicular faces	Conical	Spherical
<b>Parameter</b>					
Centerline-to-face angle, $\alpha$	65.3°	68°	35.2644°	—	—
Area (projected), A(d)	24.56d <sup>2</sup>	24.504d <sup>2</sup>	2.5981d <sup>2</sup>	$\pi a^2$	$\pi a^2$
Volume-depth relation, V(d)	8.1873d <sup>3</sup>	8.1681d <sup>3</sup>	0.8657d <sup>3</sup>	—	—
Projected area/face area, A/A <sub>f</sub>	0.908	0.927	0.5774	—	—
Equivalent cone angle, $\psi$	70.32°	70.2996°	42.28°	$\psi$	—
Contact radius, a	—	—	—	d tan $\psi$	$(2Rd-d^2)^{1/2}$

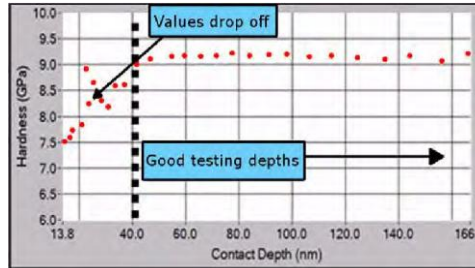
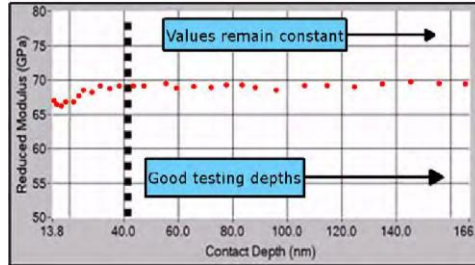
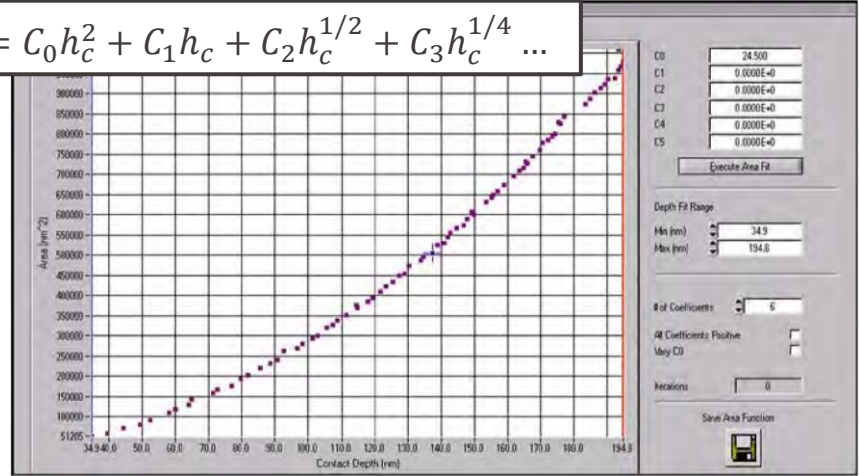
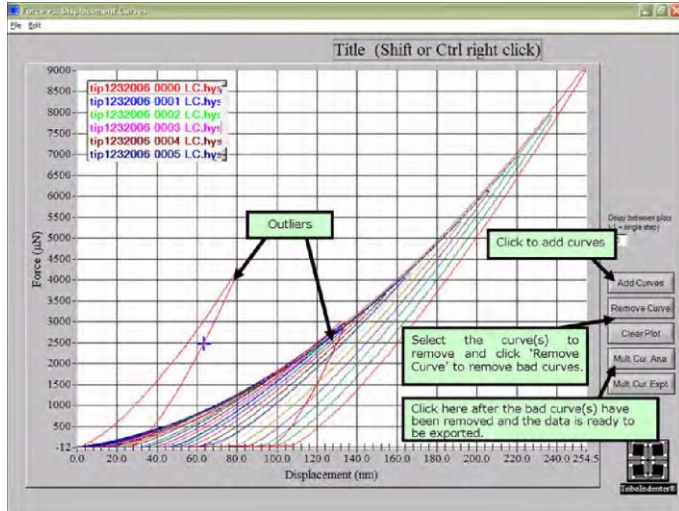
How to select the correct indenter tip –Support note, Agilent Technologies

- Spherical and flat-punch indenters are ideal for soft materials (polymers, biological samples);

# Know your tip...

## Tip area function

$$A_c = C_0 h_c^2 + C_1 h_c + C_2 h_c^{1/2} + C_3 h_c^{1/4} \dots$$



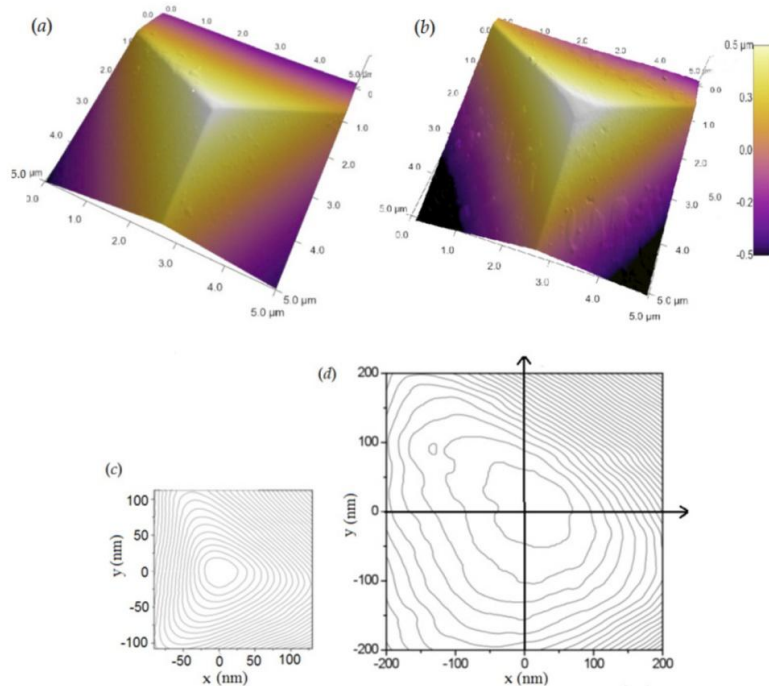
Reduced modulus stays constant even below the tip curvature;

Hardness fluctuates below the tip curvature;

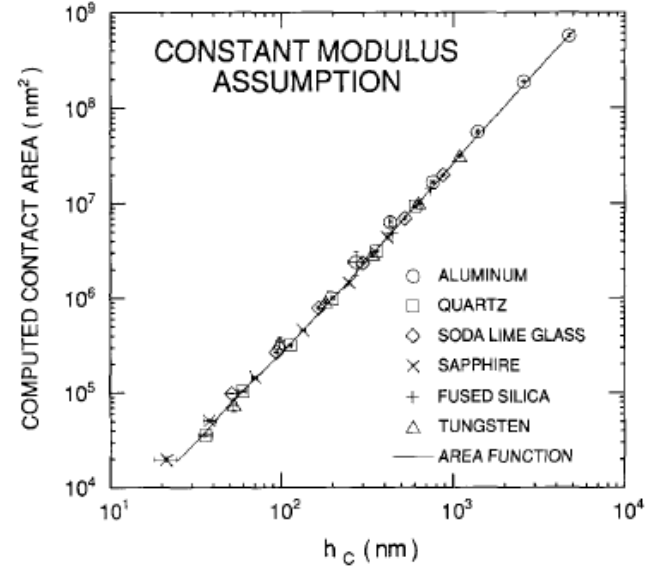
# Know your tip...

## Non-ideal tip geometry

Direct method: AFM



## Indirect method: Frame Compliance & Tip Area Function Calibration



$$A_c = \frac{\pi}{4} \frac{1}{E_r^2} \frac{1}{(C - C_f)^2}$$

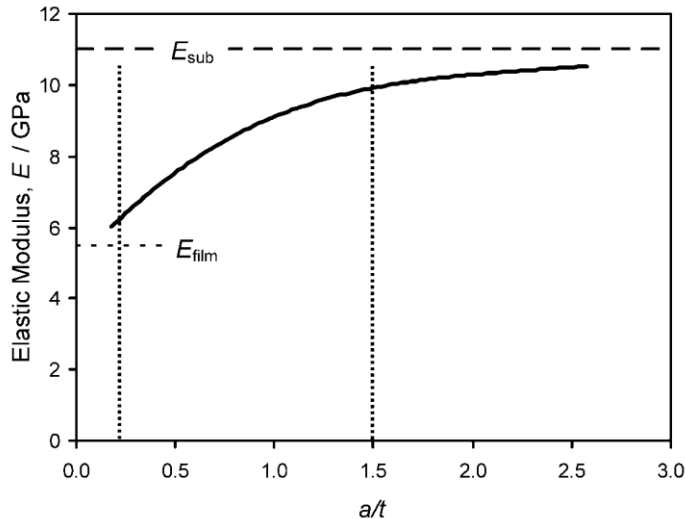
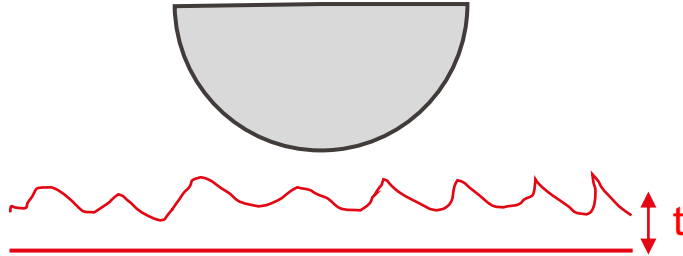
$$A_c = C_0 h_c^2 + C_1 h_c + C_2 h_c^{-1/2} + \dots$$

Ma, Li, et al. "Effect of the spherical indenter tip assumption on the initial plastic yield stress." *Nanoindentation in Materials Science* (2012): 25-52.

W.C. Oliver and G.M. Pharr, *Journal of Materials Research* Vol. 7 p1564 (1992)

# Know your sample...

## Surface roughness



Mushy layer model consists of a soft layer on top of the bulk which represents the roughness.

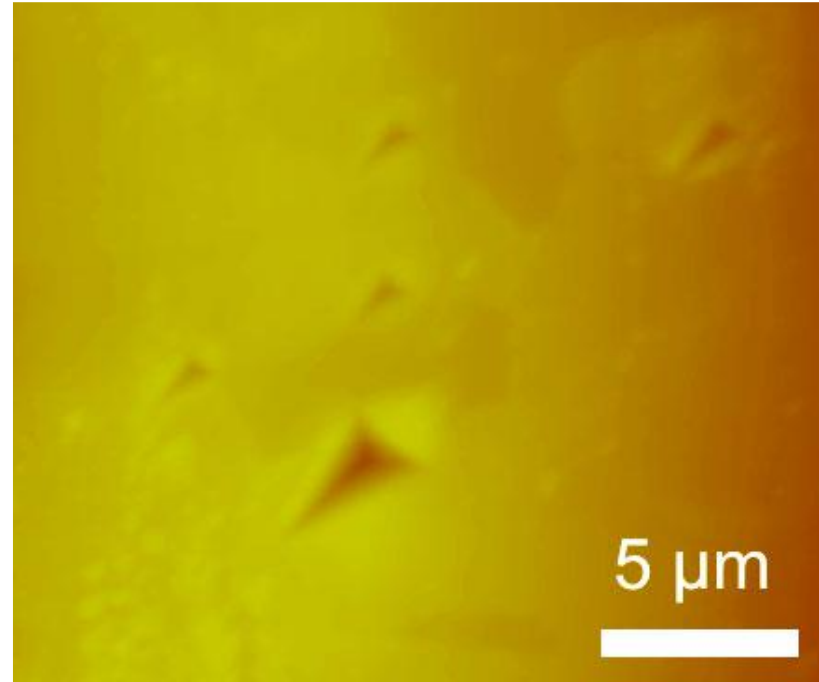
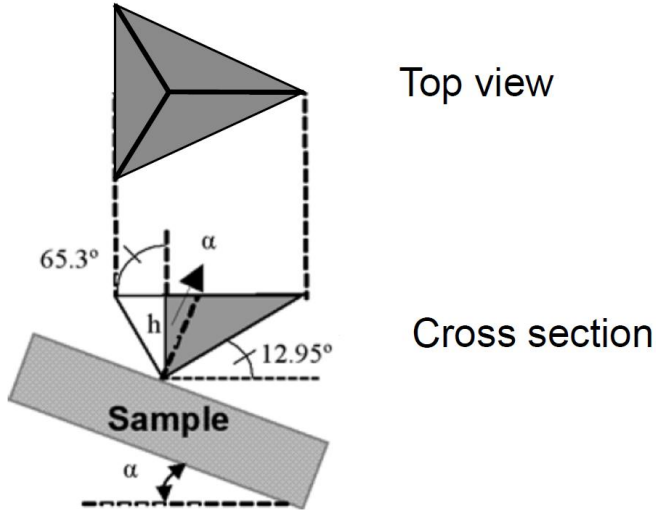
- At  $h < 2t$ , the influence of roughness is significant;
- At  $h > 10t$ , the influence of roughness is negligible;

## Embedding depth

The general rule is that **the smaller** is the **compliant layer** underneath the sample **the better**. In case of embedded samples, the backside should be removed through machining to minimize this layer.

# Know your sample...

## Tip – sample (mis)alignment

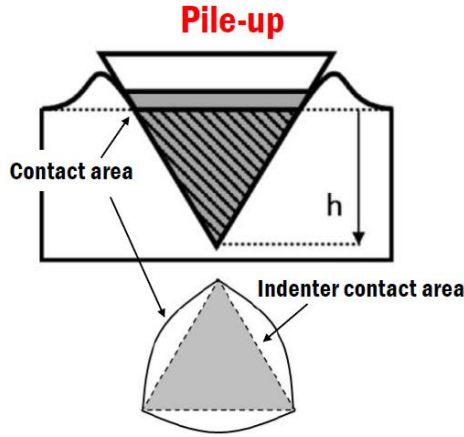




The contact area will be distorted and will differ from the calculated one, since the latter was calibrated on a flat sample.

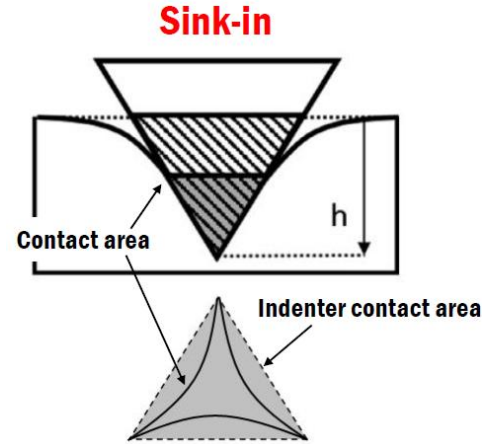
- Misalignments  $> 3^\circ$  lead to unacceptable error ( $> 5\%$  error on hardness);
- **Misalignments  $< 1^\circ$**  are acceptable;

## Pile-up & sink-in

McElhane, K. W., Joost J. Vlassak, and William D. Nix. "Determination of indenter tip geometry and indentation contact area for depth-sensing indentation experiments." *Journal of Materials research* 13.5 (1998): 1300-1306.

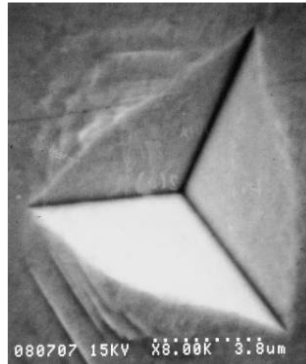


 Effective projected area between indenter and measured sample  
 Calculated projected area using measured depth  $h$



Work-hardened Cu

Annealed Cu



Displaced volume is pushed out;

Real contact area is larger than the measured;

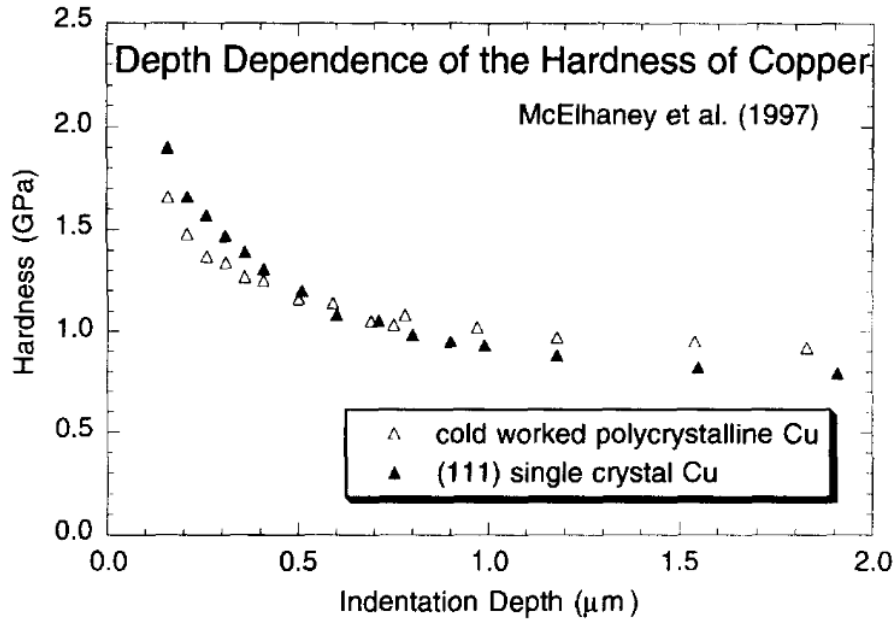
Specific to materials with low strain hardening rate;

Displaced volume accommodated mainly by far-field elastic displacements;

Real contact area is smaller than measured;

Specific to materials with high strain hardening rate;

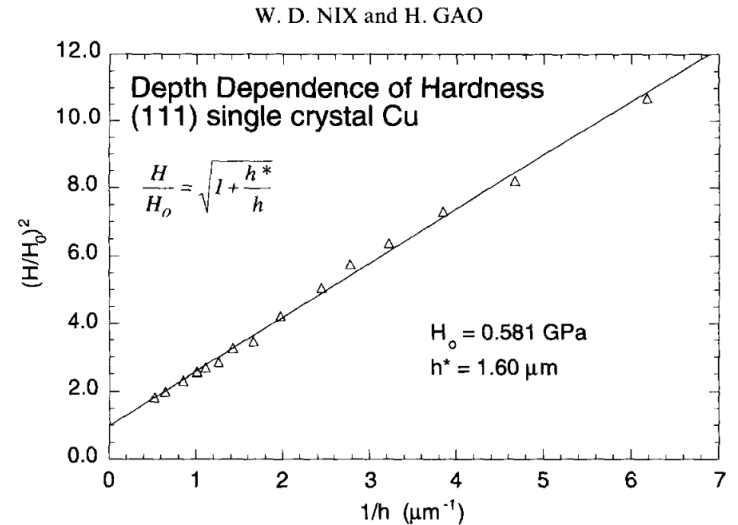
## Indentation size-effect (ISE)



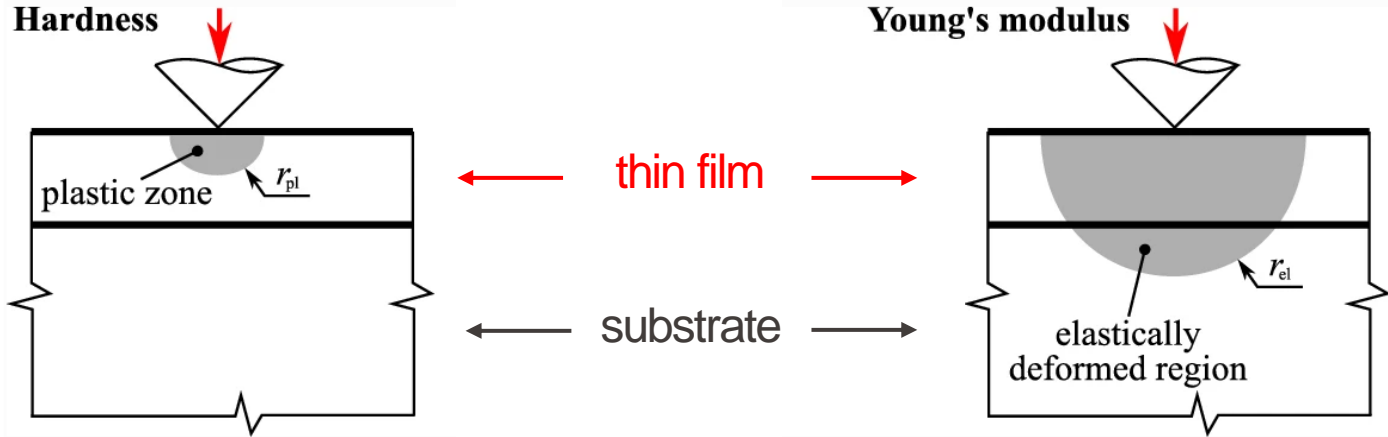
Indentation size-effect is the depth-dependence of the hardness observed in various of materials due to different localized plasticity mechanisms.

In metals, it is often attributed to the hindered movement of dislocations at the initiation of plasticity. It is highly dependent on the initial dislocation density (Nix & Gao, 1998).

$$\frac{H}{H_0} = \sqrt{1 + \frac{h^*}{h}}$$



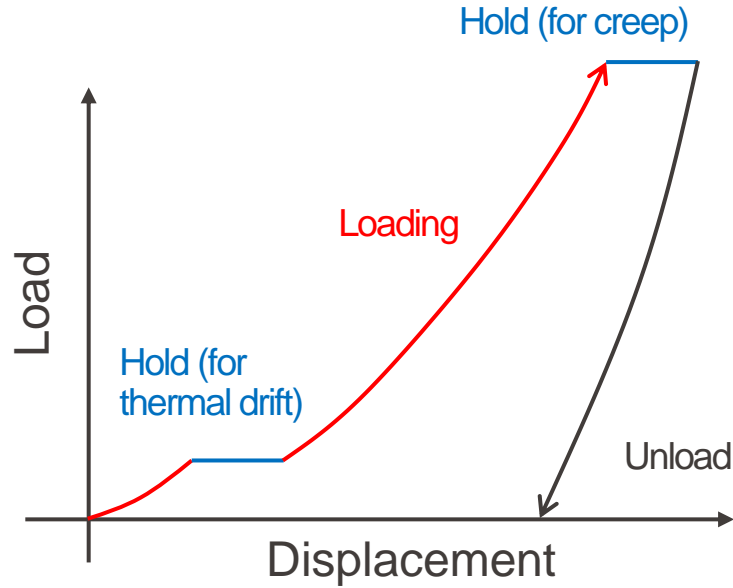
## Thin films



- Short-ranged plastic zone;
- Bückel (1953):  $H$  can be measured from indents made to **10% or less of the film thickness**;
- 10% rule was originally deduced for very thick layers (i.e.  $8 \mu\text{m}$ ) on steel;
- Elastic zone is long-ranged, much larger than the plastic zone;
- Bull (2019):  $E_r$  can be measured from indents made to **1% or less of the film thickness**;
- Equations to correct for substrate elasticity contributions when measuring  $E$  on thin films have been proposed (King, 1987 and Hay & Crawford, 2010)

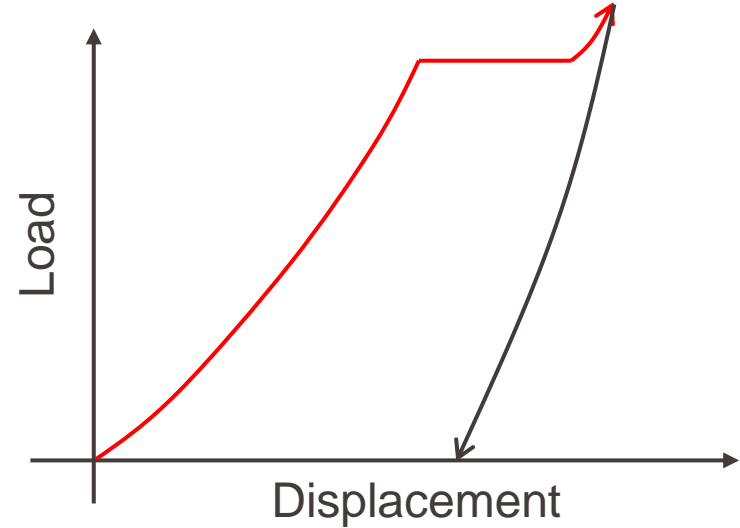
# Testing strategies

## Hardness & modulus



- Assess thermal drift and creep;
- Control load rate to assess strain rate sensitivity;
- Check elastic modulus for signs of pile-up or sink-in;
- Indent to different depths for instrument response or potential size effect;

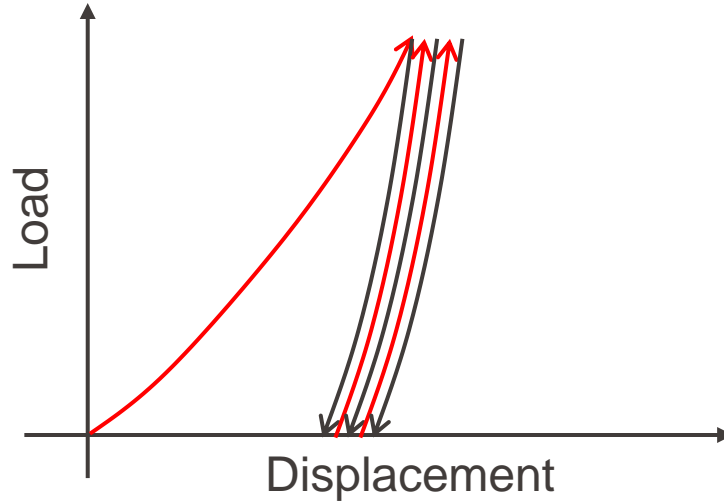
## Fracture like tests (fracture, phase transformation, strain burst)



- Cracking – sharp indenter;
- Crushing – punch indenter;
- Elastic response will be characteristic to the event;
- Many tests are required for statistical significance;

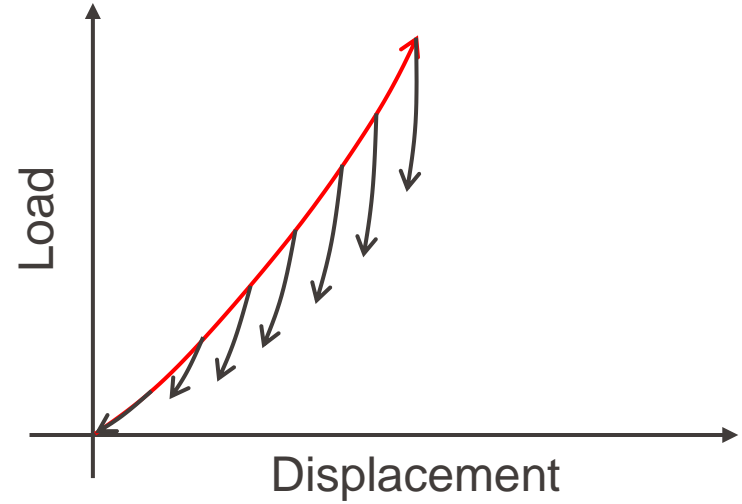
# Testing strategies

## Fatigue tests (low cycle)



- Fully or partially unloaded;
- Sharp or spherical indenter;
- Stresses can change sign underneath the indenter;

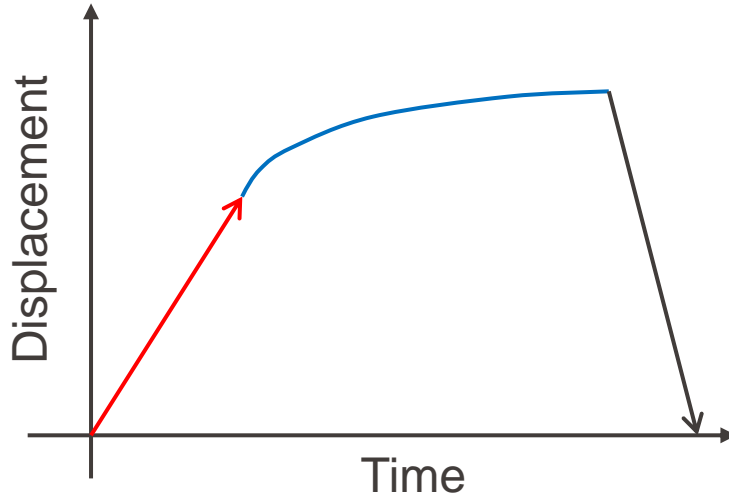
## Elastic – plastic behaviour



- Partitioning between elastic and plastic load;
- Monitoring elastic response;
- Indentation stress – strain curves can be obtained using spherical indenters;

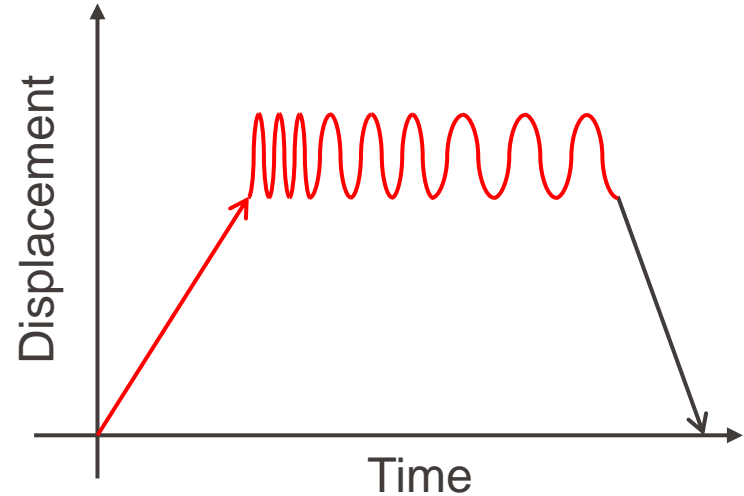
# Testing strategies

## Ramp & hold



- Punch indenter for viscoelasticity;
- Load rapidly at controlled rate;
- Hold constant force to assess time dependent response;

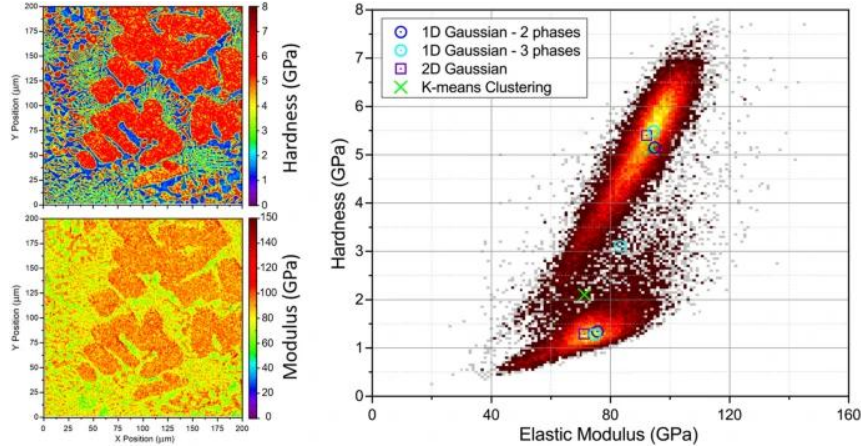
## Ramp & frequency sweep



- Punch indenter for viscoelasticity;
- Load rapidly at controlled rate;
- Oscillate the force to assess frequency dependent response;

# Current research topics

## “Mechanical microscopy”: mapping

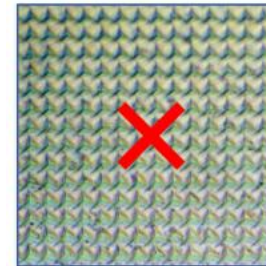


Berkovich indenter: leave at least  $10 \times h_{max}$  spacing in between indents to avoid overlap of plastic zones;

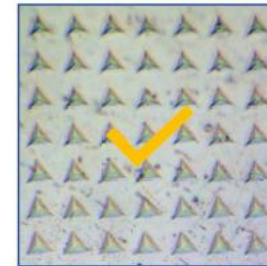
Phani, P. Sudharshan, and W. C. Oliver. "A critical assessment of the effect of indentation spacing on the measurement of hardness and modulus using instrumented indentation testing." *Materials & Design* 164 (2019): 107563.

Besharatloo, Hossein, and Jeffrey M. Wheeler. "Influence of indentation size and spacing on statistical phase analysis via high-speed nanoindentation mapping of metal alloys." *Journal of Materials Research* 36.11 (2021): 2198-2212.

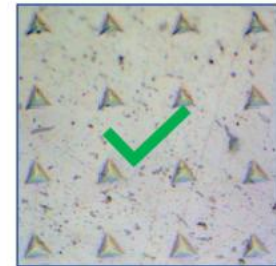
- High-resolution nanoindentation mapping is one of the mainstream techniques;
- It can be used to identify the new phases based on their mechanical properties;
- Once coupled with other techniques like EBSD and EDX it can provide crucial correlative information;



$5 \times h_{max}$



$10 \times h_{max}$



$20 \times h_{max}$

# Current research topics

High – strain rate nanoindentation:

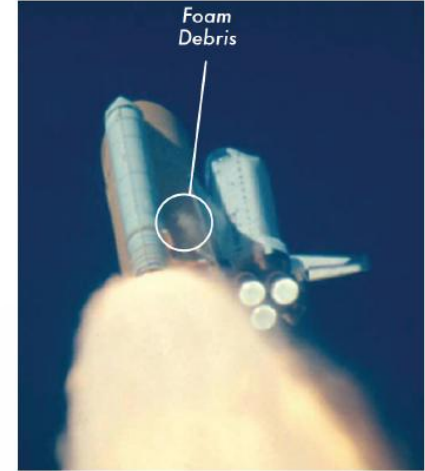
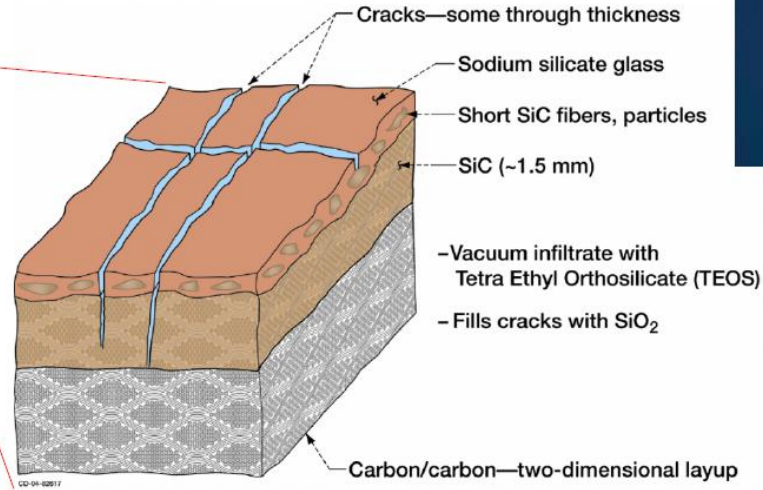
## COLUMBIA

ACCIDENT INVESTIGATION BOARD

“The basic material properties [...] were not characterized for high strain rate loadings typical of an impact.” (p. 79)

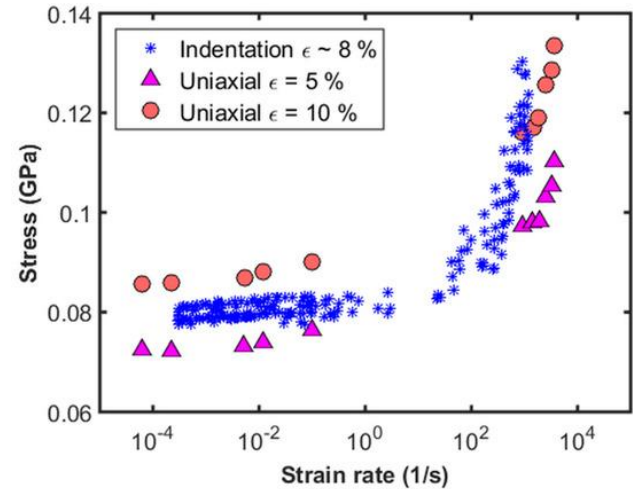
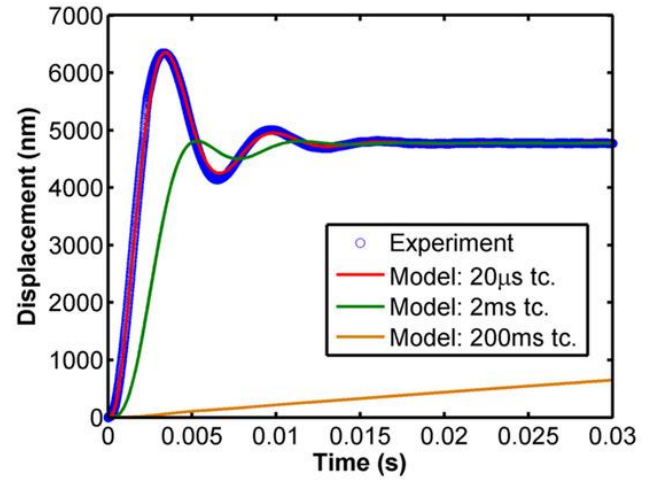
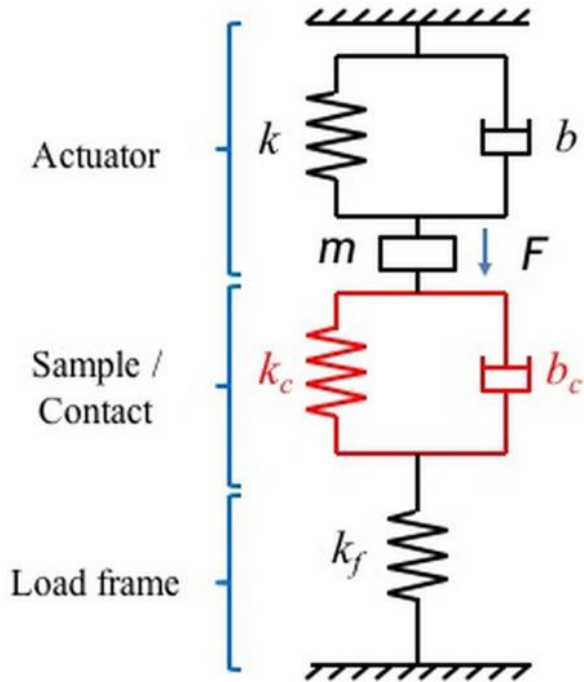


RCC panel



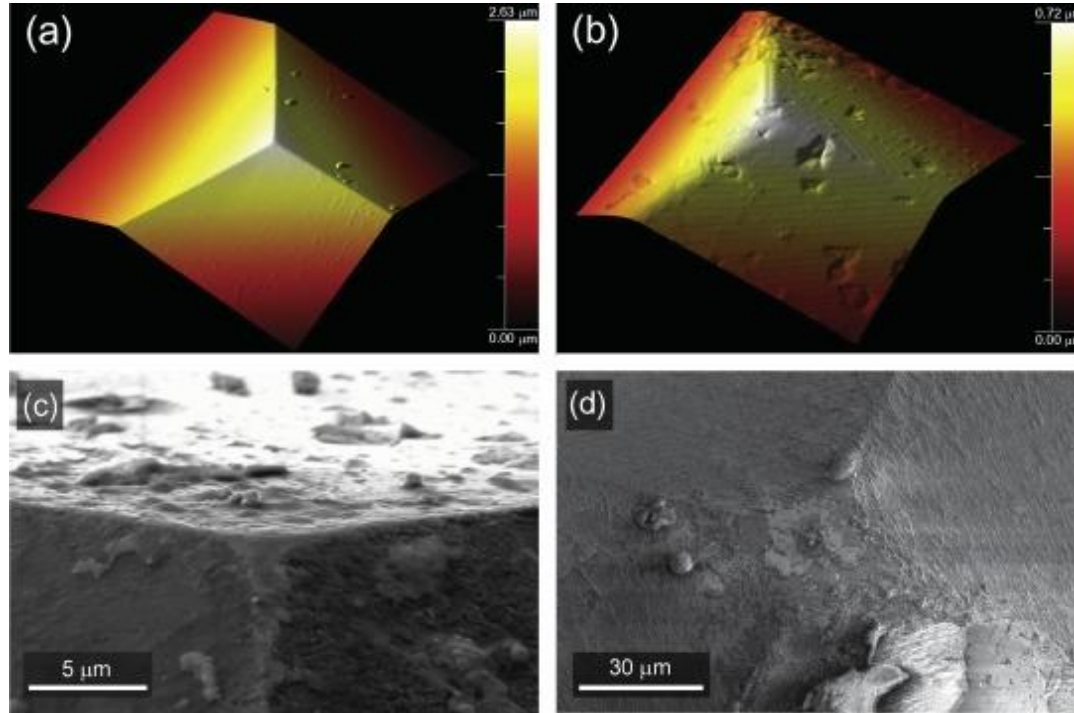
# Current research topics

## High – strain rate nanoindentation



# Current research topics

## High temperature testing



- (a) Undamaged diamond Berkovich tip after long term usage at  $< 400$  °C;
- (b) Diamond Berkovich tip in commercial argon at  $900$  °C after 90 minutes;
- (c) cBN Berkovich tip after 1000 indents into W between  $20$  °C and  $700$  °C;
- (d) Diamond Vickers tip after 100 indents into steel between  $100$  °C and  $600$  °C;

Wheeler, J. M., et al. "High temperature nanoindentation: The state of the art and future challenges." *Current Opinion in Solid State and Materials Science* 19.6 (2015): 354-366.

# CCMX 2026 Nanoindentation Course

February 11 – 13, 2026



Dr. Nicholas Randall  
(Alemnis)



Prof. Andy Bushby  
(Queen Mary University of London)

# Summary

- ✓ Over 100 years of evolution from Hertz (1882) to Oliver Pharr (1992) have made nanoindentation a robust and versatile technique to characterize micron scaled volumes of material;
- ✓ During nanoindentation, we obtain a load displacement curve, from which we can derive the  $E_r$  and  $H$  of the material by analyzing the unloading elastic response;
- ✓ We have discussed the fundamental setup related, tip related and sample related pitfalls of nanoindentation;
- ✓ We have established testing strategies for testing different mechanical properties in various samples;
- ✓ Some of the current hot topics in nanoindentation are “mechanical microscopy”, high strain rate / impact testing and high temperature testing;